Egyptian Journal of Soil Science

http://ejss.journals.ekb.eg/

Soil Aggregation and Carbon Sequestration as a Result of Carbon Nanopolymers Application under an Alluvial Degraded Soil

Enas Soliman[*], **Yasmin Abdullatif, Ayman El-Ghamery** and **Mostafa M. Mansour**

Soils Department, Faculty of Agriculture, Mansoura University, Mansoura 35516, Egypt

THE SOIL'S resistance to erosion and degradation, distribution of pore sizes, carbon sequestration and the microbial community are all directly dependent on soil aggregation, particularly macro- (0.25–2.00 mm) and micro- (0.053–0.25 mm) aggregates. Therefore, this study focused on monitoring the formation of macro and micro-aggregates to determine how soil macro-structure in clay loamy soil responds to the addition of carbon nanopolymers (CNPs) as a source of organic carbon (OC) during 30 days of incubation under a constant temperature (25 °C), and further, which soil properties are primarily responsible for the accomplishment of that aim. A short-term (4 weeks) incubation experiment was conducted in the laboratory of the Soils Department, Faculty of Agriculture, Mansoura University using three carrier materials such as chitosan (CS), pectin (PC), and acacia gum (AG) which were polymerized using methacrylic acid (MAA) and loaded with three concentrations (0, 50, and 75%) of NPKCa in addition to the control (100% NPKCa) at field moisture condition. The treatments were laid out in a completely randomized design with three replications. After 30 days of incubation, the obtained results showed the ability of nano-acacia gum (NAG) at both concentrations 50 and 75% to increase the total organic carbon (TOC) by 170.30, and 182.38% respectively. In addition, nano-pectin loaded with 75% NPKCa (NPC$_{75\%}$) recorded an increase in macro-aggregates (>0.25 mm) formation with 28.84% more than the control (71.46 mm). While nano-chitosan loaded with 50% NPKCa (NCS$_{50\%}$) treatment continued to provide dissolved organic carbon (DOC) in soil with an increase of 123.33% and encouraged the formation of micro-aggregates more than macro-aggregates (>0.25 mm) which has an important role in increasing the carbon sequestration in soil. Also, the soil's high TOC and Ca^{2+} have a greater negative clay zeta potential enhancing the formation of macro-aggregates, particularly NAG and NPC. Also, NAG can increase the mean pore diameter (MPD) with an average of 10.31 μm due to its effect on soil macro-aggregates. All suggested nanopolymers succeeded in increasing the TOC content and soil quality until the end of the study period. The loading with NPK can improve the stability of CNPs at the same time it is considered slow-release fertilizers. Macro-aggregates contain younger organic material, while micro-aggregates are confined to older OC. Long-term carbon sequestration in terrestrial systems originates from TOC confinement within micro-aggregates. Therefore, the study requires more time to monitor their decomposition in different soil textures.

Keywords: Short-term pot experiment, Organic carbon, Aggregate size, Soil degradation, Soil quality.

1. Introduction

Agriculture is one of the main drivers of Egyptian economic development, contributing 11.3 % of the country's gross domestic product. The agricultural sector accounts for 28% of all jobs, and over 55% of employment in Upper Egypt is agriculture-related. The agricultural sector contributes to the Egyptian economy at two levels: (i) it ensures part of the nation's food security, and (ii) to a lesser extent, it brings in export revenues **(Devaux, 2019)**. Therefore, the present effort for sustainable agriculture focuses on changing farming practices to reduce the need for tillage and chemical inputs, preserve soil biodiversity, raise soil carbon, and improve the physical properties of the soil **(Mechri et al., 2023)**. Since soil is the most critical natural and non-renewable resource, studying, predicting and amending its degradation is considered a key task for its maintenance, achieving food security, and avoiding any decrease in economic progress rate. Therefore, land use, management techniques, and the degree of soil degradation all significantly impact soil quality.

Soil degradation is an unquestionably severe 21st century global problem. Recent data, according to some estimations, show that in arid and semi-arid areas of the world **(Allam et al., 2024)**, degraded soils amount to 3.6 out of 5.2 billion hectares, which means a reduction in ecosystem services by more than 67% **(León & Osorio, 2014)**. The most significant type of soil degradation is physical degradation, which is caused by a reduction in structural characteristics including mainly pore geometry and their continuity. It renders soil more susceptible to

compaction, crusting, reduced water movement, and soil desertification. Additionally, this type is related to the biological degradation of soil due to the loss of soil organic carbon (SOC), which lowers the soil's carbon storage, reducing soil biodiversity **(Lal, 2015; Obalum et al., 2017)**. Soil degradation is considered one of the primary environmental problems, which destroys soil carbon (C), nitrogen (N), potassium (K), calcium (Ca) and magnesium (Mg) stocks. This has a negative effect on soil fertility, productivity, and quality. This study is linked to relevant Sustainable Development Goals (SDGs) of the United Nations, No. 15 "protect, restore and promote sustainable use of terrestrial ecosystems, sustainably manage forests, combat desertification, and halt and reverse land degradation and halt biodiversity loss." The 15.3.1 goal uses soil carbon stock as an indicator to evaluate land degradation.

Agricultural soil's organic matter (SOM) changes quickly, especially in arid and semi-arid regions such as Egyptian conditions. As a result, the amount of SOC decreases in combination with decreases in the soil structural stability by breaking down macro-aggregates into micro-aggregates **(Elbasiouny & Elbehiry, 2019)**. These factors increase soil erosion and decrease the soil's ability to resist deterioration, its capacity to regulate climate change emissions, and nutrient imbalances which prevent root dispersion and growing microbial communities **(Mechri et al., 2023)**. Therefore, encouraging soil aggregation is the key to enhancing soil fertility. All these effects depended on (i) the SOC content, and (ii) the degree of clay dispersion which is used to assess the stability of soil structure in dispersive sodic soils **(Baumert et al., 2018)**.

To address these challenges, the OM is utilized which affects the soil's physical properties, *viz.* soil structure, available water capacity, water retention, thermal conductivity, infiltration, erodibility, soil aggregate formation, soil compaction, soil color, saturated and unsaturated hydraulic conductivity and soil aeration **(Beck-Broichsitter et al., 2018; El-Henawy et al., 2024)**. According to soil chemical properties, the SOM effect buffering capacity, pH, base saturation, cation exchange capacity, exchangeable cations, zeta potential, soil fertility, and nutrient release **(Sulman et al., 2018; Voltr et al., 2021)**. On the other hand, the decomposition of SOM is directly related to the emission of atmospheric carbon, leading to global climate change. Therefore, it has a great effect while studying carbon sequestration in the soil **(Lorenz & Lal, 2018)**. However, maintaining or increasing the SOM content is essential for maintaining the productivity of the agro-ecosystems **(Abdullatif et al., 2024; Schmidt et al., 2011)** including soil quality and health **(Lal, 2020)** and ensuring future food safety **(Stavi et al., 2016)**. Thus, using the regular application of organic manures can achieve long-stable yields while maintaining soil quality/health **(Menšík et al., 2019)**, but it increases the carbon dioxide (CO_2) emission in the atmosphere.

This study focuses on increasing SOC using an alternative source to organic manure like carbon nanopolymers (CNPs). These polymers are included under the engineered nanoparticles, intentionally designed at the nanoscale to offer unique properties for maintaining soil health and biodiversity **(Faizan et al, 2023; Gupta et al., 2024)**. Organic carbon represents the soil organic binding component and is involved in the formation of aggregates and soil structure **(Durigan et al., 2017; Onweremadu et al., 2007)**. In particular, there is a positive effect of the SOC found in macro-aggregates (2–8 mm) on the stability of these aggregates **(Das et al., 2014)**. It is directly related to soil aggregation since it could form an organic core surrounded by clay, silt particles, and also aggregates. These results were confirmed by **Jozedaemi and Golchin, (2024)** who found that the macro-aggregates of more than 2 mm contain 47.5 to 57.2% of the total SOC stock. Therefore, understanding the mechanisms of SOC preservation from decomposition is essential given the significance of SOC stores and their dynamics in managing climate change. It is understood that soil aggregates can effectively protect OC from microbial decomposition. Promoted micro-aggregate formation and carbon stabilization due to reduced macro-aggregate formation have been proposed to enhance carbon sequestration. The chemical connection of SOC with clay particles and its physical connection into micro-aggregates tender it has a resistance against mineralization **(Castellano et al., 2015)**, which becomes the main mechanism of SOC stabilization in the soil **(Garcia-Franco et al., 2014)** consequently increases the ability to sequestration of carbon.

The novelty area of research is related to the utilization of CNPs as a soil conditioner and a new technique to fight soil degradation. One of the selected raw materials as a carrier material in CNPs is polysaccharides that could adsorb with clay minerals and it is the most important aggregate-stabilizing agents in soil but their effectiveness is relatively short-lived **(Theng, 2012)**. It is the most prevalent of the biopolymers as well as the most abundant organic material on earth. Nanomaterial-polymerized polysaccharide-based entities have served as inventive sorbents or more effective (nano) catalysts. They can be considered one of the sources of OM in the soil and an alternative to traditional fertilization due to the possibility of loading some nutrients on them *viz.* N, P, K, and Ca. Natural polysaccharides, which are repeat units of mono-saccharides $[C_n(H_2O)_n]$ and included in this study CS, PC, and AG are now considered sustainable materials because of their exceptional structural characteristics, a source of carbon that can be incorporated into their composition, widespread availability,

nontoxicity, flexibility, and committed potentials **(Nasrollahzadeh et al., 2021)**. Furthermore, they have high adsorption capacity, biodegradability, low cost and excellent hydrophilicity because they have carboxyl (COOH-) and hydroxyl (OH⁻) groups, flexible structure of biopolymer chains that make them well-matched with the attachment to nutrients **(Dohendou et al., 2021)**. Also, the enrichment of CNPs with calcium could enhance the formation of soil aggregates. Thus understanding the relationships between soil carbon with calcium and aggregate formation **(Vargas et al., 2019)**, would help define rates and types of these CNPs.

In terms of different reviews, several studies have provided evidence supporting the use of organic fertilizers to control or reduce the impact of soil degradation, while there are a few studies that exposed the effects of CNPs in the soil as an alternative source of traditional organic materials. In addition to their OC content, it is considered natural, degradable materials and slow-release fertilizers at the same time. According to these notes, our hypothesis depends on the ability of the proposed CNPs to prevent clay dispersion by creating macro-aggregates and minimizing clay particle exposure to water, regulating CO_2 emissions and increasing the storage of SOC. For these reasons, our objectives for this study are to (i) evaluate the effect of CNPs (types and concentration of nutrients) on soil aggregates and SOC compared with traditional treatment, (ii) investigate the relationship between SOC, surface charge properties, aggregate formation and soil pores under degraded soil treated with CNPs. The results of this work will allow for improved management of degraded alluvial soil by applying CNPs which improves aggregate formation, and carbon sequestration thus improving soil sustainability.

2. Materials and methods
2.1 Materials
All used reagents were of analytical grade wherein, CS (degree of deacetylation 95%, MW 68.5 kDa) was purchased from Loba Chemie Pvt. Ltd., Mumbai, India. The PC from citrus peels, (poly-d-galacturonic acid methyl ester 80.5%, 70–140 kDa), potassium persulfate 95.8% ($K_2S_2O_8$), and methacrylic acid (MAA) 94.7% [$CH_2C(CH_3)COOH$] were purchased from Techno Pharmchem, Bahadurarh, Haryana, India. AG from acacia tree 85.0%, 250 kDa, was purchased from Oxford Lab Chem, Mumbai, India. Urea 98.9% (CH_4N_2O), mono potassium phosphate 99.9% (KH_2PO_4), and calcium chloride dehydrate 96.7% ($CaCl_2.2H_2O$) were purchased from Merck KGaA, Germany. The composition of the initial carrier materials (raw materials) is illustrated in **Table 1**.

Table 1 Chemical composition of carrier materials.

Carrier material	Molecular weight (kDa)	TC (%)	TN (%)	C:N ratio	Moisture content (%)	TS (%)
CS	50–2000	39.23	6.27	6:1	6.47	2.86
PC	50–150	35.67	0.71	50:1	5.45	2.32
AG	2000–4500	38.68	0.68	57:1	3.75	ND

CS: chitosan, PC: Pectin, AG: Acacia gum, TC: total carbon, TN: total nitrogen, C:N: carbon to nitrogen, TS: total sulphur, ND: Not detected, All analyses were carried out by Thermo Scientific Flash 2000 elemental analyzer (**ISO 10694: 1995** and **ISO 13878: 1998**), Mean values ± SD, n = 2

2.2 Preparation of CNPs loaded with NPKCa
Nano-chitosan (NCS) was prepared by polymerization using MAA in a two-step process according to **Corradini et al. (2010) and de Moura et al. (2008)**. The CS 1% (w/v) was dissolved in acetic acid (CH_3COOH) 2% (v/v) and placed on a magnetic stirrer (800 rpm) at 60 °C until it was completely dissolved. After this step, the mixture of CS and acetic acid solution was mixed with a 0.5% (v/v) MAA and left on a magnetic stirrer (600 rpm) for 12 hours at 60 °C. The solution was then given by 10 ml of $K_2S_2O_8$ (0.2 mmol) while being continuously stirred until the solution was clear without any clumps or sediments. After one hour of 70 °C magnetic stirring at 600 rpm, the polymerization was completed, producing CS/MAA nanopolymer. In the same way, NPC and NAG were prepared by polymerization using MAA in a two-step process as previously mentioned but using distilled water as a solvent instead of acetic acid, and both of them were at a concentration of 1% (w/v). There are no temperature controls during preparation, and generally, the temperature is set using an air conditioning system at 25 °C. Furthermore, all preparations at different temperatures were monitored by a thermometer to ensure no changes in the used temperature (Fig. 1).
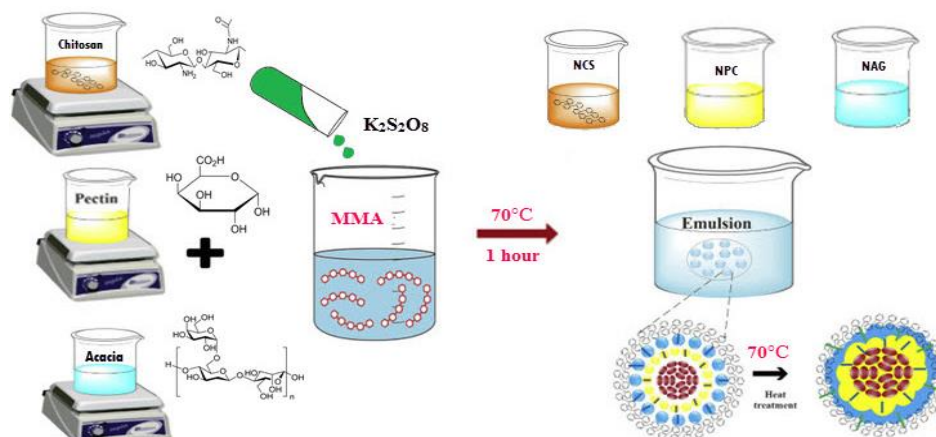
Fig. 1. The procedures for the synthesis of carbon nanopolymers.

According to the mechanism of solubility of raw materials, CS is a strong base owing to the presence of primary amino groups and becomes a polyelectrolyte when such amino groups get protonated. As a result, CS dissolves in acid-aqueous mixtures (i.e. aqueous acetic acid). While PC is mainly composed of polyagalacturonic acid (>70%) and is water soluble. When dissolved, PC decomposes rapidly by de-esterification or depolymerization. Most of the unesterified carboxyl groups in PC occur as partially ionized salts in a neutral or very slightly acid dispersion of PC molecules. Those that are ionized produce a negative charge on the molecule, which together with the hydroxyl groups causes it to attract layers of water. PC are generally hot water-soluble and often contain dextrose (a dispersion agent) to prevent lumping. AG has a highly branched molecular structure responsible for water's high solubility. It is also associated with a protein moiety, which is responsible for water's emulsifying and foaming properties.

Urea and mono potassium phosphate were used as N, P, and K sources to incorporate into the CNPs (NCS, NPC, and NAG) by dissolving in different quantities according to their concentration **(Khalifa & Hasaneen, 2018)**. Urea was added to each nano-solution separately and mixed for 30 min at 60 °C (600 rpm), then mono potassium phosphate in the same way. According to nano-calcium solutions, they were prepared separately by loading the three CNPs with $CaCl_2.2H_2O$ at a rate of 500 kg ha^{-1}, to avoid precipitation Ca by P that was added by mono potassium phosphate forming insoluble tri-calcium phosphate, then placed on a magnetic stirrer (600 rpm) at 60 °C for 30 min until completely dissolved. After preparation, the NCS was stored at room temperature, while NPC and NAG were stored in a temperature-controlled environment (4 °C) to extend their storage time and to prevent them from breaking down. Quantities of nano-solutions as the first batch were prepared and analyzed to ensure that the required properties were formed, and then they were prepared again with sufficient amounts to repeat the analyses and used in the incubation experiment. All solutions were prepared in the Lab of Soil Fertility Testing and Fertilizers Quality Control, Faculty of Agriculture, Mansoura University (accredited ISO 17025/2017).

2.3 Characterization of CNPs loaded with NPKCa

To ensure the efficacy of CNPs solution, the size and morphology of the three solutions were examined using a HRTEM JEM 2100 transmission electron microscope (TEM). The CNPs emulsions were subjected to a two-minute sonication process to enhance particle dispersion and prevent nanopolymer agglomeration on the copper grid. One drop of the nanopolymer emulsion was applied on a copper grid coated with carbon (200 mesh), and it was then allowed to dry at room temperature. The zeta potential (ZP) of CNPs suspension loaded with NPKCa in various concentrations was examined by a Zetasizer NanoZS (Malvern analyzer, Worcestershire, UK) at 25 °C. These analyses were measured at the Electronic Microscope and Molecular Imaging Unit, Faculty of Agriculture, Mansoura University. Moreover, the Fourier Transform Infrared (FTIR) spectroscopy were conducted to determine the functional groups of CNPs by Nicolet™ iS™ 10 FTIR Spectrometer, Thermo Scientific™, USA. For FTIR spectroscopy accuracy, spectra obtained from 32 scans were collected from 4000 to 400 cm^{-1} at varied spectral resolution of 8.0 cm^{-1}. Pellets made from powdered samples were created using potassium bromide (KBr) at the Spectral Analysis Unit, Faculty of Science, Mansoura University. For the KBr pellet, it was pulverized into a 200-mesh size followed by drying at 110 °C to remove any bound water molecules. Then a few drops of each nano-solution were introduced into the cell and mixed with 200 to 250 mg

of powdered KBr to have a minimum thickness of 1.5 mm and a maximum of 3 mm. Next, the sample pellet was placed into a pellet-forming die. Further, a force of 8 tons was applied under vacuum for several minutes to form a transparent sample pellet, and degassing removes the air and bound water molecules. After that, the liquid cell was properly sealed to prevent leakage and then placed in the sample holder to perform the FTIR analysis.

2.4 Incubation experiment set-up

The soil samples were collected from Mit Khamees Village, Mansoura District, Dakahlia Governorate, Egypt. The location is geographically coordinated in the Northern part of the Egyptian Nile Delta at 31°04'N latitude and 31°34'E longitude. Most soil properties in the study site are similar to which was confirmed by previous studies on the same site (**Mansour & Soliman, 2022; Soliman et al. 2019**). To ensure the accuracy of the experiment in representing the study site, forty soil samples were randomly selected from the topsoil (0–30 cm) using a global positioning system (GPS). These samples covered an area of two hectares; the representative sample was created from all soil probes by mixing soil samples thoroughly using a suitable mechanical mixer and spreading into a thin layer on a tray of stainless steel that would not influence the composition of the sample. The soil was separated into four equal portions (quadrants). Two of the four portions were combined diagonally, rejecting the other two. This procedure was repeated until the desired amount of soil was obtained (**ISO 11464, 2006**). Furthermore, a disturbed soil sample was taken from each site to analyze the soil's physical properties before the experiment. The soil samples were air-dried, passed through a 2 mm sieve, and analyzed. The initial soil properties with their standard methods are illustrated in **Table 2**.

An *in vitro* incubation study was done to clarify the effect of CNPs on some physical properties of the soil and to monitor the CNPs decomposition in an alluvial soil for a short-term (30 days). The experiment was carried out using clay loamy soil at the Lab of Soil Department, Faculty of Agriculture, Mansoura University. It was laid out in a completely randomized design with three replications under controlled conditions. The treatments involving three CNPs for example NCS, NPC, and NAG, in combination with three concentrations (0, 50, and 75%) of the fertilizers recommended doses for the sugar beet plant, additionally to the control (100% NPKCa) treatment with a total number of ten treatments.

Table 2 Initial physical and chemical properties of the studied soil.

Soil characteristics	Abbrev.	Unit	Value
Saturation percentage	θ_{SP}	%	54.79
Filed capacity	θ_{FC}	%	27.40
Wilting point	θ_{WP}	%	13.70
Bulk density	ρ_b	$Mg\ m^{-3}$	1.22
Real density	ρ_s	$Mg\ m^{-3}$	2.20
Total porosity	Φ	%	44.50
Hydraulic conductivity	K_S	$m\ day^{-1}$	0.30
Particle size distribution	Sand	%	33.00
	Silt	%	29.00
	Clay	%	38.00
	Texture class		Clay loamy
Potential of hydrogen ions†	pH	-	7.38
Electrical conductivity††	EC	$dS\ m^{-1}$	3.18
Calcium carbonate	$CaCO_3$	%	1.07
Organic matter	OM	%	1.71

† measured in soil paste, †† measured in soil paste extract, mean values ± SD, n = 2

The details of incubation experiment treatments involving the concentrations after loading with N, P, K, and Ca are elucidated in **Table 3**. The soil was packed layer by layer with consistent tapping and watering, in plastic cans (5 cm high and 6 cm in diameter) with a soil height of 4 cm and 138 g weight to reach the final bulk density of 1.22 $Mg\ m^{-3}$. The CNPs loaded with NPKCa were added to cans at the beginning of the experiment at a rate of 1.5% (v/w), in comparison with the control treatment (100% NPKCa) which received the conventional fertilizers at the recommended doses of the Agriculture Ministry of Egypt for the sugar beet plant. Firstly, CNPs loaded with NPK were added, then after 2 days, CNPs loaded with Ca were added to avoid any reaction between them.

Table 3 The details of incubation experiment treatments.

Treatments		NPKCa concentration (ppm)	Addition rate of CNPs to soil (v/w)	Diameter of CNPs by TEM (nm) after loading with	
				NPK	Ca
Control	100%	Conventional fertilizers	–	–	–
NCS	0%	–	1.5%	22.98–88.59	
	50%	350:65:80:90	1% NPK + 0.5% Ca	11.10–47.65	6.90–28.89
	75%	525:100:120:135	1% NPK + 0.5% Ca	12.39–54.97	29.54–14.91
NPC	0%	–	1.5%	20.61–89.29	
	50%	350:65:80:90	1% NPK + 0.5% Ca	14.92–46.23	3.60–6.65
	75%	525:100:120:135	1% NPK + 0.5% Ca	15.41–58.15	13.45–16.87
NAG	0%	–	1.5%	21.13–77.92	
	50%	350:65:80:90	1% NPK + 0.5% Ca	8.18–22.25	8.24–21.88
	75%	525:100:120:135	1% NPK + 0.5% Ca	10.78–38.68	11.87–19.79

NCS: nano-chitosan, NPC: nano-pectin, NAG: nano-acacia gum, N: nitrogen, P: phosphorus, K: potassium, Ca: calcium, CNPs: carbon nanopolymers, TEM: transmission electron microscope.

The NPKCa for all treatments were calculated at the rate of 70:70:60 kg ha^{-1} for N, P_2O_5 and K_2O, respectively. The conventional fertilizers for control treatment were urea (46%N), calcium super phosphate (15% P_2O_5, 4.5% CaO), and potassium sulfate (48% K_2O). The cans were placed in an incubator at a temperature of 25 °C and the soil moisture was maintained at 80% of the water holding capacity (WHC). And to keep it constant at this level, the loss of weight was compensated by adding distilled water. This rate could promote the presence of an equal portion of air and water for soil microorganisms. The soil samples were taken after incubation periods of 14 and 30 days and were frozen till carrying the different analyses.

2.5 Soil analysis

The collected soil samples were prepared according to **ISO 11464 (2006)**. The TOC was measured according to **ISO 10694 (1995)** using the Thermo Scientific Flash 2000 elemental analyzer. The total carbon was assumed to be equal to the TOC with negligible inorganic carbon concentration because of the decreasing soil calcium carbonate ($CaCO_3$) content of less than 2% **(ISO 10694, 1995)**. The DOC was extracted according to **(Jones & Willett, 2006)**, and then estimated by wet oxidation method according to **(Walkley & Black, 1934)**. The saturated hydraulic conductivity (K_S) was estimated by the constant head permeameter method **(Reynolds et al., 2002)**. The bulk density (BD) was estimated using the cylinder method **(Hillel, 1982)**. Dry sieving was used to measure the aggregate size distribution using sieves of 1.00, 0.50, 0.25, 0.106, and 0.053 mm, according to **(Dane & Topp, 2002)**. The mean weight diameter (MWD) was calculated using the following equation:

$$MWD = \sum_{i=1}^{n} d_i\, w_i \qquad (1)$$

where *di* is the mean diameter of any size range of aggregates separated by sieving (mm), and *wi* is the weight of the aggregates in that size range as a fraction of the total dry weight of the sample (g).

The mean pore diameter (*d*) was calculated according the equation of **(Dielman & De Ridder, 1972)** using the saturated hydraulic conductivity (K_S - m day^{-1}).

$$d = 6.177637\sqrt{K_s} \text{ (for water at 20 °C)} \qquad (2)$$

Electrophoretic mobility measurements were examined at two periods 14 and 30 days to determine the ZP of soil samples. The light scattering was measured using user-supplied or calculated input parameters for fluid type including [viscosity (0.8872), dispersant RI (1.33), and dispersant dielectric constant (78.5), temperature (25 °C)], in addition to particle size, pH, and by measuring the direction and velocity of the particle movement via light scattering. The technique of ZP was used as an illustrated characterization of CNPs loaded with NPKCa section. After adding CNPs to the soil, we measured the ZP of particles obtained by centrifuging the suspension. All the measurements were carried out by obtaining a concentration of 500 mg soil per L^{-1} deionized water. For the measurement, a 50 mg soil sample was transferred into a volume of distilled water and the soil particles were mixed homogeneously using a magnetic stirrer for 15 min. The solution's specific conductivity determines the voltage that has to be applied. The movement of the particles is seen under a microscope and the amount of time it takes a particle to traverse a certain distance in micrometers is calculated. To minimize reading error, a minimum of 10 particles are tracked and their average time is calculated. The pH that was observed after the ZP

measurement was recorded as the final pH and it was carried out using a pH-meter (Jenway 3505 pH/mV/Temperature Meter). The electrical charge was measured as a function of pH, and the adsorbed amount of nanopolymer on the surface of colloid particles by a Zetasizer NanoZS (Malvern analyzer, Worcestershire, UK) at a scattering angle of 90° and a temperature of 25 °C.

2.6 Statistical analyses

To assess the statistical significance of CNPs application on different soil parameters, a one-way analysis of variance (ANOVA) was performed, using the least significant difference (LSD). In order to improve our results, we used ANOVA with Duncan's significance testing ($p<0.05$) as a Post Hoc test to examine the effects of the variables soil carbon forms, ZP, porosity, and MPD. The significant variables (soil carbon forms i.e., TOC and DOC) that affect MWD, aggregates more and less than 0.25 mm were identified using a linear regression. The statistical analyses and the Pearson correlation coefficients to display the relationships between all the soil parameters were performed using the IBM SPSS Statistics Software (v22, 2013). The figures and FTIR curves were plotted using OriginPro Software (v9.5.1.195, 2018).

2.7 Quality assurance and quality control

All the chemicals for the equipment calibration purchased from Merck KGaA, Germany. The range of the adjusted average recovery was 99.25 to 101.13%. The accuracy of TOC was confirmed by calibrating the apparatus using a certified reference sample (aspartic acid, $C_4H_7NO_4$). The pH-meter was calibrated by two Merck standard buffer solutions at (20 °C): di-sodium hydrogen phosphate/potassium hydrogen phosphate (7) and boric acid/potassium chloride/sodium hydroxide (10), both of them traceable to SRM from NIST and PTB. The results of ZP presented herein are within 20% of true ZP. Before any testing, the particle size and ZP of the standard provided by the manufacturer were measured at room temperature. Our results were within 2% of 200 nm for particle size and measured -73 ± 7 mV for ZP, which indicated that the device was operating properly. Based on this procedure, we determined that ± 7 mV is the standard for precision among the sets of replicated measurements. The samples were repeated three times (repeatability test) to determine the precision of the analytical methods, and the results were expressed as the standard deviation (SD). Additionally, all analyses were validated using different ways e.g. quality control materials, control charts (X, R and shewart), intermediate checks on measuring equipment, a laboratory control sample (LCS) and testing of blind samples. The external calibration of the equipment is required to establish the metrological traceability of the obtained results. The Calibrations are carried out by the National Institute of Standards (NIS) with equipment traceable to international standards. These calibrations aimed to achieve accuracy or measurement uncertainty which affects the validity of results. The frequency of calibration is altered upon review of the manufacturer's manual and/or calibration results if it is observed any deviation of results. Calibration certificates of the used equipment include reference values and correction factors; we ensured that these values were implemented in our results. Furthermore, internal calibrations were applicable using reference standards calibrated by an accredited lab and/or traceable to National/International Standards or using certified reference material. In addition, outliers in set measurements were identified and handled in the data analysis by the "Q" Test which was used to confirm acceptance or rejection of the obtained data.

3. Results

3.1 Transmission electron microscope (TEM) of CNPs

The CNPs prepared by polymerization between carrier materials and MAA substrates are highly crystalline, circular nanopolymers **(Fig. 2)**. The average diameter of different CNPs is shown in **Table 3**, where the CNPs produced spherical shapes and sizes of about 55.79, 29.38, and 49.53 nm for NCS, NPC, and NAG, respectively using the TEM micrographs. These values depend on various reaction conditions, which lead to various distributions. The mean diameter of all the CNPs in suspension was decreased with the addition of the different nutrient compounds. The addition of calcium chloride was more effective on CNPs solution stability than urea and monopotassium phosphate. The size of CNPs solution was higher with the addition of Ca^{2+} than with the addition of NPK, due to the higher anion charge from the second than the first one. Thus, the average sizes of CNPs loaded with 50% Ca^{2+} were recorded at 17.90, 5.13, and 15.06 nm for the NCS, NPC, and NAG, respectively.
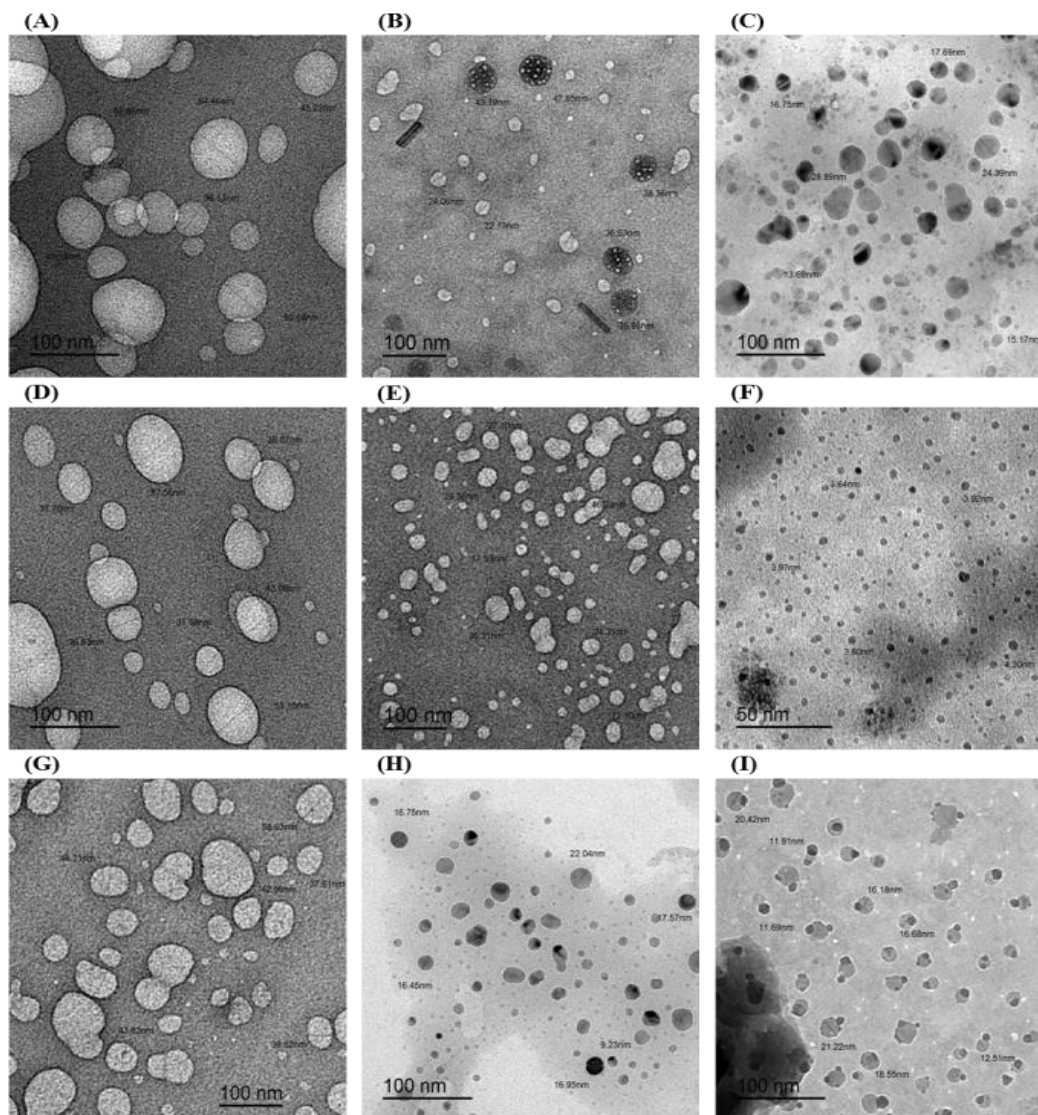
Fig. 2. Representative TEM images of CNPs solutions. Images show (A): NCS alone or with, (B): NPK$_{50\%}$, (C): Ca$_{50\%}$, (D): NPC alone or with, (E): NPK$_{50\%}$, (F): Ca$_{50\%}$, (G): NAG alone or with, (H): NPK$_{50\%}$, and (I): Ca$_{50\%}$.

On the other hand, the estimated functional groups of the three CNPs by the FTIR spectrum **(Fig. 3)** were approximately similar. The FTIR spectrum obtained for the NCS, NPC and NAG has characteristic peaks: 3500-3100 cm^{-1} corresponding to the stretching of the NH$_2$ (primary amine) and OH (intermolecular bonded) groups; 2080–2105 cm^{-1} corresponding to the N=C=S (isothiocyanate); 1683–1633 cm^{-1} corresponding to the C=O group of amide I; 1083–1020 cm^{-1} due to the stretching of C–O (alcohol) and 670–690 cm^{-1}, due to the stretching of C=C (alkene). Additionally, it is observed that the band at 1600–670 cm^{-1} which appears in all CNPs, begins to change due to loading nutrients. For instance, 1600 cm^{-1} (group –COO–) and 1500 cm^{-1} (group –NH$_3^+$) indicate MAA and carrier materials interaction. Significant differences can be observed comparing the spectrum obtained for CNPs$_{0\%}$ (carbon nanopolymers without loading nutrients) with those obtained from the loaded CNPs with urea, mono potassium phosphate and calcium chloride. It is observed that there was no significant change in the structure of the CNPs with the incorporation of N, P, K, and Ca fertilizers.

3.2 Soil zeta potential

Data in **Table 4** showed that the NCS solution has a positive charge at the pH ranging from 2.78 to 4.09. After 14 days of addition, the NCS treatments have a negative charge in the pH range of 8.6 to 9.17 and this charge is due to the high soil pH. The charge of NCS treatments decreases with the increase of the rate of loaded NPKCa. NPC showed the same trend, but it did not change much when using the high rate of loaded NPKCa$_{75\%}$. NAG reduced the value of ZP, but it increased again when using the high rate of loaded NPKCa$_{75\%}$. It was observed that after 30 days, the ZP of the soil colloid surface decreased in all nanopolymer treatments as compared to 14 days. The NPKCa$_{75\%}$ treatment recorded the highest ZP value in all CNPs.
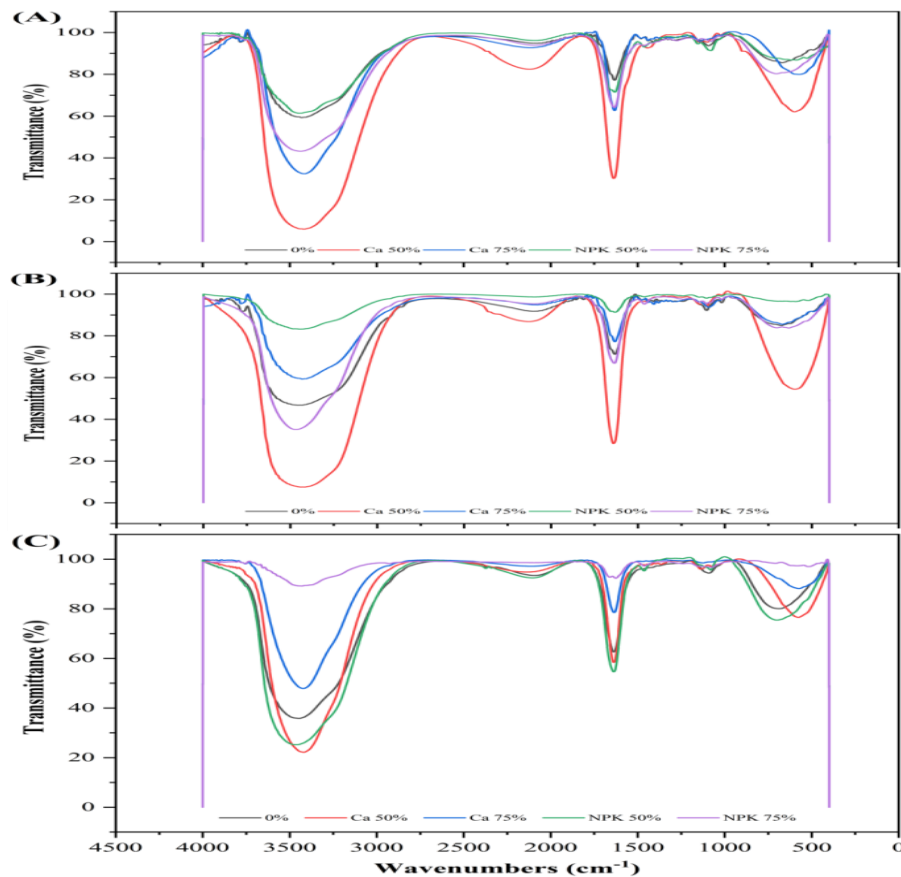
Fig. 3. FTIR transmittance spectra of CNPs and CNPs with [urea (N-NH$_2$CONH$_2$) + mono potassium phosphate (P, K - KH$_2$PO$_4$)] and CNPs with [calcium chloride (Ca - CaCl$_2$)] at two rates (50 and 75%).
Images show (A) NCS, NCS with [urea (N-NH$_2$CONH$_2$) + mono potassium phosphate (P, K - KH$_2$PO$_4$)] and with [calcium chloride (Ca - CaCl$_2$)] at two rates (50 and 75%), (B) NPC, NPC with [urea (N-NH$_2$CONH$_2$) + mono potassium phosphate (P, K - KH$_2$PO$_4$)] and with [calcium chloride (Ca - CaCl$_2$)] at two rates (50 and 75%), and (C) NAG, NAG with [urea (N-NH$_2$CONH$_2$) + mono potassium phosphate (P, K - KH$_2$PO$_4$)] and with [calcium chloride (Ca - CaCl$_2$)] at two rates (50 and 75%).

Table 4. Zeta potential of the CNPs and the incubated soil after 14 and 30 days.

Treatments		ZP of CNPs solution (mV) after loading with				ZP of the incubated soil (mV) after			
		NPK		Ca		14 days		30 days	
		Value	pH	Value	pH	Value	pH	Value	pH
Control	100%	–	–	–	–	-19.53ab	8.30	-22.77e	9.08
NCS	0%	36.07a	4.09	36.07a	4.09	-22.68bc	9.17	-12.13bc	8.87
	50%	25.90b	3.81	12.00b	2.78	-18.07a	9.10	-12.97bc	8.72
	75%	6.27c	3.93	3.68d	2.93	-30.75f	8.60	-13.43bc	8.91
NPC	0%	-17.27e	3.15	-17.27e	3.15	-27.60ef	7.75	-8.30a	8.40
	50%	-21.00f	3.32	10.27bc	2.14	-25.07cde	8.47	-11.53b	8.26
	75%	-13.17d	3.34	6.25cd	2.00	-27.17bcd	8.00	-14.50cd	8.27
NAG	0%	-15.57e	3.50	-15.57e	3.50	-27.00de	7.67	-17.23d	8.07
	50%	-11.07d	3.52	3.67d	2.88	-23.23c	7.90	-13.97bc	8.01
	75%	-11.53d	3.61	2.33d	2.93	-24.10cd	7.30	-17.10d	8.03
LSD (0.05)		2.29**	–	4.69**	–	3.20**	–	2.91**	–

NCS: nano-chitosan, NPC: nano-pectin, NAG: nano-acacia gum, ZP: zeta potential, CNPs: carbon nanopolymers, pH: potential of hydrogen ions, LSD: least significant difference test, mean values followed by different letters were significant when $p<0.05$ according to the Duncan test, mean values ± SD, n = 3

3.3 Effects of CNPs on the formation of soil aggregates
The application of CNPs showed a significant effect ($p<0.05$) on soil aggregate formation after 14 and 30 days of incubation (**Table 5**). After 14 days of addition, NAG is considered the highest nanopolymer in the macro-

aggregates formation (>1.00 mm), followed by NPC. Nano-acacia gum loaded with 75% NPKCa (NAG$_{75\%}$) recorded an increase in macro-aggregate formation with 49.66% more than the control (26.89%). However, NCS encouraged the creation of micro-aggregates <0.25 mm. All CNPs have a high MWD compared to the control. The loading of CaCl$_2$ on the NAG and NPC increased its effect on the formation of macro-aggregates, while Ca^{2+} did not give this effect when loaded on NCS. In addition, the MWD was significant in all treatments compared to the control at both incubation periods. After 14 days of incubation, NAG treatments recorded the highest MWD (mm) with a range of 20–22%, more than the control. After 30 days, the unloaded nano-acacia gum (NAG0%) gave the greatest value of MWD with 31%, followed by NPC75% (29%). NCS treatments recorded an obvious increase with a range of (17–19%) compared to the first period (6–10%).

Table 5. Effects of CNPs on the formation of soil aggregates after 14 and 30 days of incubation.

Treatments		Aggregate size distribution (%) after 14 days of incubation						MWD (mm)
		>1.000†	1.00–0.50	0.50–0.25	0.25–0.106	0.106–0.053	<0.053	
Control	100%	26.89f	29.90a	22.53bcd	11.93ab	6.60a	2.15a	0.50e
NCS	0%	31.60d	28.23bc	24.33ab	11.03bc	4.49b	0.33b	0.53d
	50%	30.14e	27.79cd	24.77a	12.58a	4.1bc	0.63b	0.52d
	75%	34.19c	27.03de	23.93abc	11.5abc	3.09bcd	0.28b	0.55c
NPC	0%	34.51c	27.49c	23.67abc	10.88bcd	2.85cd	0.17b	0.56c
	50%	37.63b	25.91f	22.7abcd	10.29cd	3.35bcd	0.13b	0.58b
	75%	36.89b	28.76b	21.74cd	9.41de	2.87cd	0.34b	0.58b
NAG	0%	39.13a	29.61a	20.88d	8.12e	2.10d	0.17b	0.60a
	50%	39.41a	26.42ef	21.74cd	9.47de	2.80cd	0.17b	0.60a
	75%	40.23a	28.49bc	20.96d	8.04e	2.17d	0.14b	0.61a
LSD (0.05)		1.15**	0.80**	2.20*	1.54**	1.56**	Ns	0.017**
		Aggregate size distribution (%) after 30 days of incubation						
Control	100%	28.54e	25.69d	17.24c	14.12a	8.19a	6.24a	0.48e
NCS	0%	34.38d	27.50c	23.91a	10.73b	3.34b	0.16cd	0.56cd
	50%	34.09d	28.63b	23.60a	11.24b	2.32cd	0.13cd	0.56cd
	75%	36.16c	28.16bc	23.83a	5.93f	2.13cd	0.15cd	0.57bc
NPC	0%	30.25d	28.45bc	24.11a	9.95bc	3.01bc	0.25b	0.56cd
	50%	36.44c	29.10b	23.85a	8.11cde	2.29cd	0.21bc	0.58b
	75%	39.83b	31.56a	20.69b	9.59bcd	1.86d	0.15cd	0.62a
NAG	0%	42.72a	29.00b	19.50b	6.79ef	1.89d	0.12d	0.63a
	50%	33.68d	28.80b	24.78a	9.91bc	2.68bcd	0.16cd	0.55d
	75%	37.35c	28.52bc	23.95a	7.95de	2.05cd	0.20bcd	0.59b
LSD (0.05)		1.66**	1.04**	1.42**	1.93**	1.00**	0.08**	0.016**

NCS: nano-chitosan, NPC: nano-pectin, NAG: nano-acacia gum, MWD: mean weight diameter, LSD: least significant difference test, ns: non-significant, mean values followed by different letters were significant when *p*<0.05 according to the Duncan test, mean values ± SD, n = 3, † aggregates size (mm).

3.4 Soil carbon forms

Data in **Figs. 4 and 5** showed a significant effect of CNPs on TOC and DOC at 0, 14, and 30 days. **Fig. 5** shows the initial values of DOC in the studied soil at the beginning of the incubation. Some CNPs treatments caused a slight increase in DOC as compared to the control, then all treatments decreased gradually with time. Moreover, TOC increased after the addition of CNPs compared to the control treatment, then decreased with time in all treatments. The highest TOC value was recorded by nano-pectin without nutrients (NPC$_{0\%}$, 1.34%) with a rate of 104.68% more than the control. After 14 days of incubation, the nano-chitosan loaded with 50% NPKCa (NCS$_{50\%}$) and 75% (NCS$_{75\%}$) were the highest treatments in TOC content, these increases were 74.18 and 72.59%, respectively. For DOC, NAG$_{75\%}$ was the greatest treatment with a rate of 132.27% followed by both nano-acacia gum loaded with 50% NPKCa (NAG$_{50\%}$) and NCS$_{50\%}$ with 113.65% as compared to the control. After 30 days, NAG$_{75\%}$ and NAG$_{50\%}$ were the highest treatments in TOC with 170.30 and 182.38%, respectively. NCS$_{50\%}$ treatment continued in providing DOC in soil with an increase of 126.34% more than the control treatment. These results may be attributed to the high carbon content of CS (39.23%) followed by AG (38.68%) compounds as illustrated in **Table 1**. After 30 days, the results revealed that larger aggregate-size fractions >0.25 mm had a greater amount of TOC than smaller aggregate-size fractions <0.25 mm particularly in NAG followed by NPC.
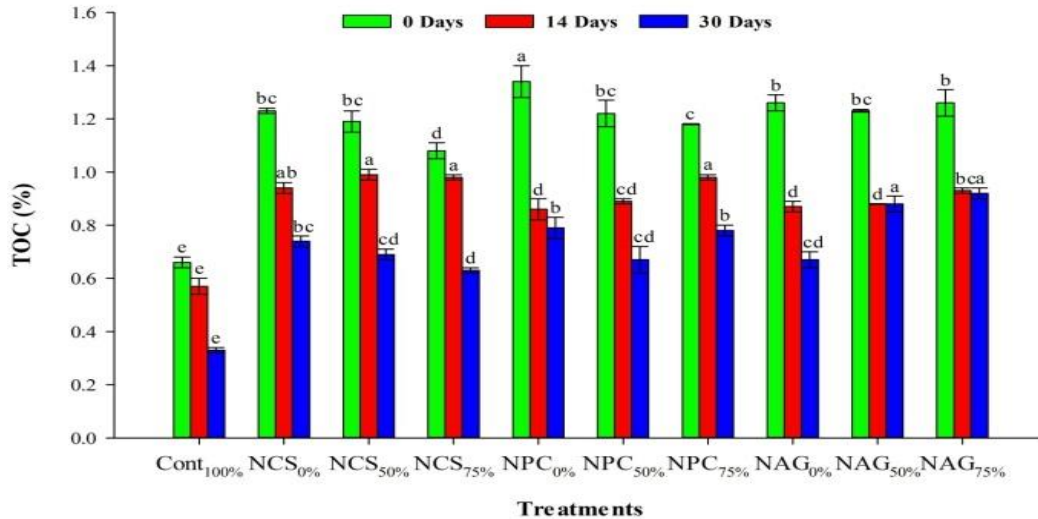
Fig. 4.Effect of CNPs application on TOC content (%).

Cont: control, NCS: nano-chitosan, NPC: nano-pectin, NAG: nano-acacia gum, TOC: total organic carbon, LSD (0.05) for TOC at 14 and 30 days = 0.022** and 0.029** respectively, Dissimilar letters were significantly different at $p<0.05$ according to the Duncan test, Bars on the columns stands for ± standard deviation (SD).

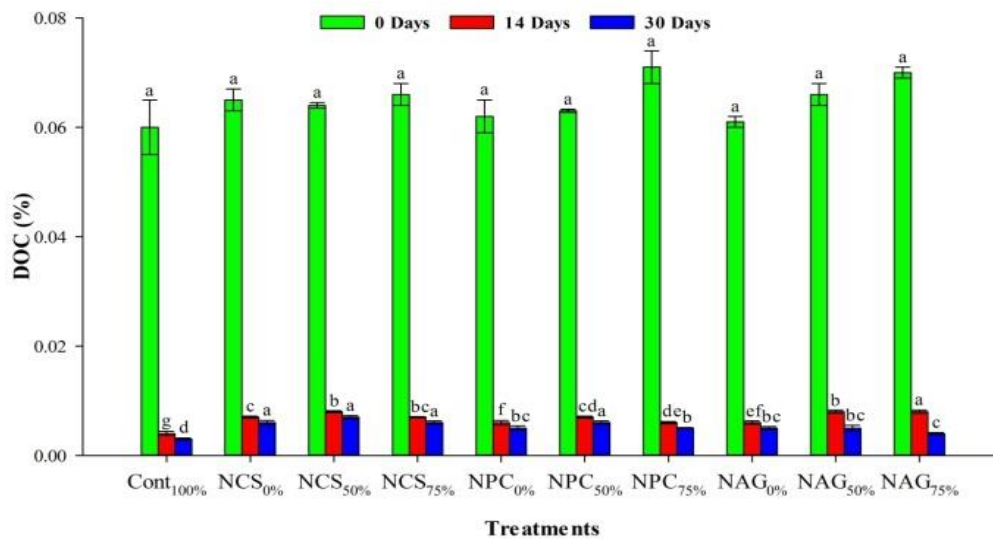**Fig. 5 Effect of CNPs application on DOC content (%).**

Cont: control, NCS: nano-chitosan, NPC: nano-pectin, NAG: nano-acacia gum, DOC: dissolved organic carbon, LSD (0.05) for DOC at 14 and 30 days = 0.022** and 0.029** respectively, Dissimilar letters were significantly different at $p<0.05$ according to the Duncan test, Bars on the columns stands for ± standard deviation (SD).

Table 6 shows the relationship between the soil carbon forms and the formation of aggregates which were expressed in our research by aggregates >0.25, aggregates <0.25, and MWD (mm) using the linear regression equations.

### 3.5 Soil porosity and mean pore diameter

Soil high in organic carbon content (SOC) has a low bulk density (BD) and a high porosity, indicating that it is less compacted **(Guo et al., 2019)**.

Table 6. Linear regression equations between soil carbon and aggregation.

| Treat.	After 14 days of incubation	R²
NCS	MWD = 0.0824 TOC + 0.4533	0.63
	MWD = 7.7778 DOC + 0.4744	0.42
	Aggregates >0.25 (mm) = 11.418 TOC + 72.894	0.81
	Aggregates <0.25 (mm) = -11.418 TOC + 27.106	0.81
NPC	MWD = 0.2085 TOC + 0.383	0.96
	MWD = 28.421 DOC + 0.3916	0.89
	Aggregates >0.25 (mm) = 0.0478 TOC - 3.226	0.98
	Aggregates <0.25 (mm) = -20.524 TOC + 32.169	0.98
NAG	MWD = 0.3243 TOC + 0.3165	0.98
	MWD = 25.455 DOC + 0.4145	0.83
	Aggregates >0.25 (mm) = 0.0326 TOC - 2.0121	0.96
	Aggregates <0.25 (mm) = -29.396 TOC + 37.345	0.96
	After 30 days of incubation	
NCS	MWD = 0.2141 TOC + 0.4146	0.88
	MWD = 22.778 DOC + 0.4172	0.89
	Aggregates >0.25 (mm) = 38.989 TOC + 59.626	0.87
	Aggregates <0.25 (mm) = -38.989 TOC + 40.374	0.87
NPC	MWD = 0.243 TOC + 0.4039	0.79
	MWD = 37.895 DOC + 0.38	0.66
	Aggregates >0.25 (mm) = 40.182 TOC + 59.11	0.88
	Aggregates <0.25 (mm) = -40.182 TOC + 40.89	0.88
NAG	MWD = 0.1478 TOC + 0.4591	0.39
	MWD = 92.479 DOC - 16.447	0.98
	Aggregates >0.25 (mm) = 28.762 TOC + 64.799	0.72
	Aggregates <0.25 (mm) = -28.762 TOC + 35.201	0.72

NCS: nano-chitosan, NPC: nano-pectin, NAG: nano-acacia gum, MWD: mean weight diameter, TOC: total organic carbon (%), DOC: dissolved organic carbon (%), R^2: regression coefficient.

This hypothesis did not occur when applying the CNPs to the degraded alluvial soil which caused an increase in BD and decreased the porosity significantly **(Figs. 6 and 7)**. NAG recorded the highest value of BD ranging from 1.36 to 1.40 Mg m^{-3} and the lowest in porosity ranging from 36.50 to 38.09% at both periods of incubation as compared to the control. It is noted from **Table 7** that all CNPs treatments displayed a statistically significant effect ($p<0.05$) on K_S and MPD.
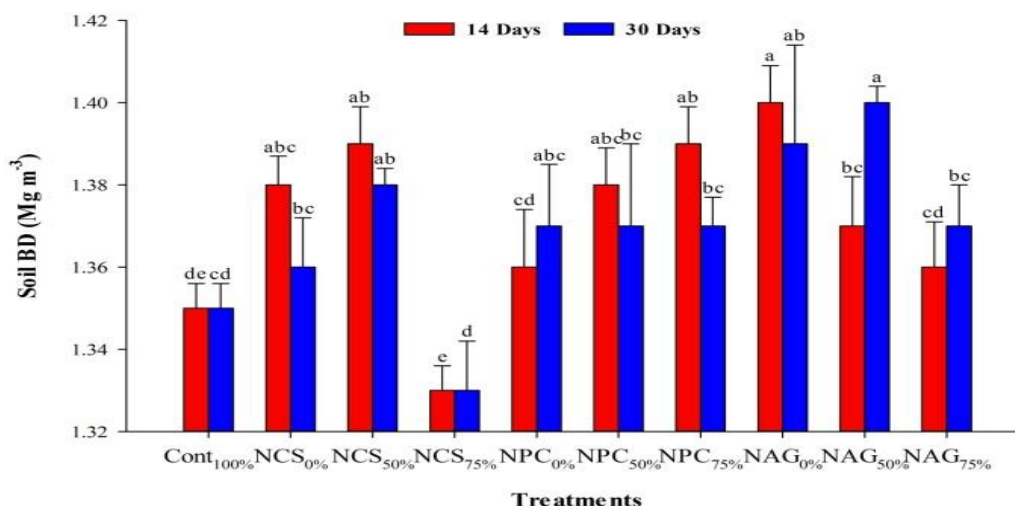
Fig. 6 Effect of CNPs application on soil BD after 14 and 30 days.

Cont: control, NCS: nano-chitosan, NPC: nano-pectin, NAG: nano-acacia gum, BD: bulk density, LSD (0.05) for bulk density at 14 and 30 days = 0.022** and 0.029** respectively, Dissimilar letters were significantly different at $p<0.05$ according to the Duncan test, Bars on the columns stands for ± standard deviation (SD).

After 14 days, $NAG_{75\%}$ was the highest CNPs in water flow, as a result of increasing the MPD, followed by $NCS_{75\%}$. Furthermore, there is a positive correlation (0.85, 0.91 and 0.94) between DOC and MPD for NCS, NPC and NAG, respectively. After 30 days, NAG treatments continued their trend of increasing K_S and MPD.
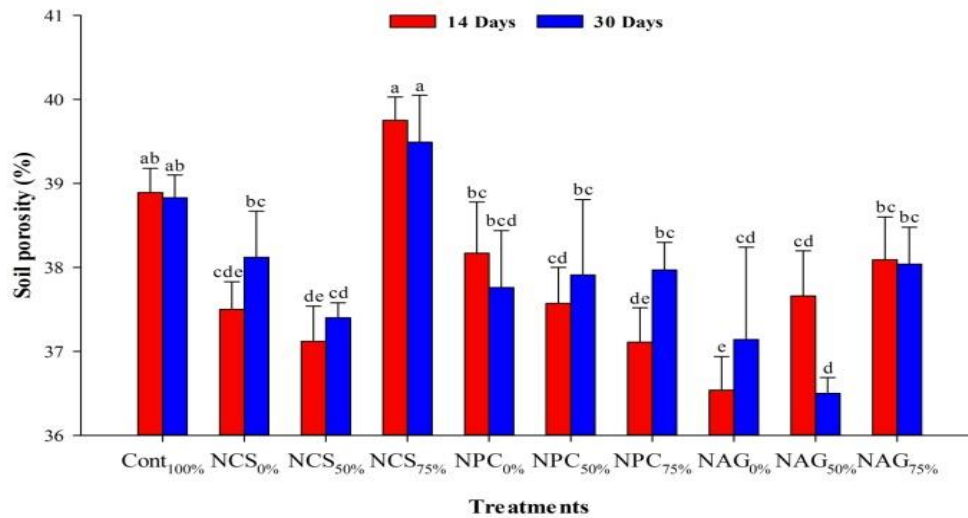
Fig. 7. Effect of CNPs application on soil porosity after 14 and 30 days.
Cont: control, NCS: nano-chitosan, NPC: nano-pectin, NAG: nano-acacia gum, LSD (0.05) for porosity at 14 and 30 days = 0.97** and 1.33** respectively, Dissimilar letters were significantly different at $p<0.05$ according to the Duncan test, Bars on the columns stands for ± standard deviation (SD).

Table 7 Effect of CNPs on water flow and MPD.

Treatments		After 14 days of incubation		After 30 days of incubation	
		K_S (m day^{-1})	d (µm)	K_S (m day^{-1})	d (µm)
Control	100%	0.56f	4.60g	0.86c	5.70c
NCS	0%	1.40e	7.29f	2.41ab	9.59ab
	50%	1.41e	7.33ef	2.28ab	9.32ab
	75%	1.93ab	8.58ab	2.68a	10.11a
NPC	0%	1.40e	7.31ef	1.99b	8.72b
	50%	1.54de	7.65def	1.99b	8.70b
	75%	1.67cd	7.98bcd	2.30ab	9.75ab
NAG	0%	1.64cde	7.91cde	2.76a	10.26a
	50%	1.89bc	8.48bc	2.76a	10.23a
	75%	2.17a	9.09a	2.87a	10.45a
LSD (0.05)		0.25**	0.63**	0.60**	1.19**

NCS: nano-chitosan, NPC: nano-pectin, NAG: nano-acacia gum, K_S: hydraulic conductivity, d: mean pore diameter, LSD: least significant difference test, mean values followed by different letters were significant when $p<0.05$ according to the Duncan test, mean values ± SD, n = 3

A strong relationship between porosity and mean pore diameter was observed in all CNPs up to $NPKCa_{50\%}$ concentration. In contrast, the high rate of NPKCa (75% RD) has the opposite effect on porosity. The correlation coefficients between both parameters when using NCS were -0.98 & -0.83, 0.64 & 0.98 for NPC, and -0.32 & -0.95 at 14 and 30 days after incubation.

4. Discussion
Typically, the suggested carbon nanopolmers (CNPs) are produced as colloidal aqueous suspensions, and particle size diversity is caused by the polymerization process. External factors like pH, the concentration of nanopolymers, temperature, and ionic strength significantly affect the suspension's rheological characteristics as well as the particles' extent of individualization **(Shafiei-Sabet et al., 2014)**. These results may be due to the negative charge of the ester (R–CO–OR) groups on the nanoparticle surface producing electrostatic repulsion forces that keep the solution stable. More generally, their surface chemistry governs their propensity to aggregate. For instance, by adding electrolytes, the surface charges of the particles are covered, lessening the electrostatic repulsion that keeps CNPs from clumping together. Depending on the amount of electrolyte added, these results in either a decrease or an increase in the prepared particle size **(Corradini et al., 2010; Kaushik et al., 2015)**. The suggested CNPs are significant natural polymers that have a lot of carboxyl and hydroxyl

functional groups. These groups can interact electrostatically with organic and metal cations, as well as be altered chemically to create hybrid and composite materials (**Corradini et al., 2010; Li et al., 2022**). Additionally, they have a vital role in the interaction with clay colloids, which means that they can remain in the soil and resist degradation for a long time.

The effect of CNPs on the aggregation of the charged clay loamy soil through clay ZP is not fully clear. For this reason, one of the objectives of this paper was to study the CNPs' effect on the clay ZP and soil aggregation accordingly. The prepared nano-solutions with loading with NPK rates significantly affected their ZP values. The obtained data are confirmed by **Corradini et al., (2010)** who indicated that the cationic properties of CS in the pH range of 2 to 5.5 are responsible for the positive loading of the NCS nanoparticles, as indicated by the positive values of the ZP. Furthermore, it is observed that the charge of CS decreases with the increase in the rate of loaded NPKCa. The negative charge of the NPC solution increased when loaded with 50% NPK and decreased when the rate was 75%. The negative charge of the NAG solution decreased when loading with any rate of NPKCa.

The results showed the appearance of negative charges after adding all the CNPs treatments to the clay loamy soil, also it led to significant changes in the charge of the colloid surface. The isoelectric point of CNPs systems, where the positive and negative charges are equal, is pH = 5.5. It is a sign that the system is somewhat unstable at this pH. The surface of the NCS is negatively charged at pH values greater than 5.5, which can be attributed to the ionization of MAA's carboxyl groups and the neutralization of CS's $-NH_2$ groups (**Corradini et al., 2010**). These results were related to the results of (**He et al., 2021**) who found that greater negative clay ZP was related to aromatic carbon functional groups, higher SOM content and greater concentrations of Ca^{2+} and Mg^{2+} than the control. As a result, clay ZP and higher SOC enhanced water-stable macro-aggregates by releasing less amount of clay particles lower than 10 μm.

The addition of CNPs was significant in forming soil aggregates and increasing the value of MWD compared to the control at both incubation periods. According to **Tisdall & Oades (1982)** and modified by **Ghezzehei (2012)**, they found that micro-aggregates (the initial unit of aggregation) consist of associations of free primary particles together by persistent binding agents like polyvalent cations, metal oxy(hydro)oxides, Ca & Mg carbonates and organic molecules. On the other hand, macro-aggregates (>0.25 mm) are formed from the combination of micro-aggregates (0.25 mm), particulate organic materials and sand, which are then bound by transient binding agents e.g. PC and AG. The carbon-to-nitrogen ratio in OM is crucial to control microbial activity. High C:N ratio in organic compounds, such as NPC and NAG >30:1, decompose more slowly because they don't contain enough nitrogen to meet the development requirements of the microbes that cause the degradation but promote the formation of extracellular enzymes that mineralize native SOC, primarily aggregate-unprotected carbon (**Dijkstra et al., 2013**). While organic materials having a low C:N ratio, such as NCS (<30:1) will decay very rapidly in the soil, releasing large amounts of CO_2, organic molecules, and some nutrients for the soil (**Jílková et al., 2020**) which can be an adhesive material for micro-aggregates, consequently, increasing the carbon sequestration and stability in the soil (**Zhu et al., 2024**).

Abdullatif et al., (2024) and **Guber et al., (2005)** referred to an important positive connection between MWD and the actual amount of >0.25 mm aggregates. The great effect of $NAG_{75\%}$ may be due to the composition of the raw material (AG) which consists of high-molecular weight polysaccharides and their Ca, Mg, and K salts in addition to loaded Ca^{2+}. For this reason, there is a greater concentration of Ca^{2+}. These amounts of Ca^{2+} are important to the formation of macro and micro-aggregates and are more effective after irrigation which acts as a potential cationic bridge between the negatively charged clay particles (**Nasrollahzadeh et al., 2021; Yamaguchi et al., 2004**) and organic colloids' surfaces (**Bronick and Lal 2005**) and promotes the formation of soil aggregates (**Liu et al., 2023**). A high saturation of clay particles with these cations helps the organic-mineral complex to remain more flocculated and condensed as well as reducing the efficiency of microbial and enzymatic attacks (**Xie et al., 2024**), contributing to the sequestration of carbon. Also, polysaccharides are hydrolysis, producing three major fractions of proteins and polysaccharides (**Musa et al., 2018**). These fractions besides their nano size may be another reason for this effect.

Increasing soil organic carbon content is the key to soil improvement, the application of CNPs caused an increase in TOC (**Fig. 8A**). The amounts of macro-aggregates (>1.00 mm) had a significant positive correlation with the TOC (r = 0.996) content and with DOC (r = 0.91). For MWD, the results recorded a positive correlation (r = 1.00 and 0.91) with DOC, and TOC respectively. The results of this study indicate that NAG is the perfect treatment for increasing TOC and DOC which creates macro-aggregates >1.00 mm till 30 days of incubation. The formation of macro-aggregates is considered important in preserving SOM (**Sekaran et al., 2021; Wang et al., 2019**), which is a requirement for soil health in agricultural soils (**Ghezzehei, 2012**). Macro-aggregates play a significant role in TOC storage and its sequestration. Because macro-aggregates create an environment that facilitates interactions between clay particles and the TOC, protection by macro-aggregates becomes weak. Micro-aggregates have been considered a key factor in forming new macro-aggregates due to the protection of intra-aggregate TOC. Therefore, the direction of micro-aggregate formation is helpful for long-term soil carbon sequestration (**Abdullatif et al., 2024; Zhou et al., 2020**).

The availability of polyvalent cations, such as Ca^{2+}, is an important factor in the chemical protection of TOC. Calcium exerts an influence on organo-mineral complexation and its stability is observed mainly at the micro-aggregate level (Abd El-Halim, 2019; **Vargas et al., 2019; Xie et al., 2024**). Higher carbon accumulated in macro-aggregates could be due to the lower decomposable soil organic materials associated with these aggregates and also the direct contribution of CNPs to the stability of macro-aggregates resulting in only C-rich macro-aggregates being able to resist their breakdown due to CNPs additions in the soil. The results from the present study agree with the results of **Mirzaei Aminiyan et al., (2015); Tripathi et al., (2014)**.

Numerous studies support the connection between enhanced aggregate formation and inputs of organic materials **(Karami et al., 2012; Soliman & Mansour, 2024)**. Organic inputs added to the soil give substrate materials for soil fungi, physically encouraging soil particles into macro-aggregates. When fungi grow more quickly and enmesh soil particles with their hyphae, they exude polysaccharides onto mineral surfaces that can further form macro-aggregates **(Gazzè et al., 2013)**. The CS is considered an anti-fungal compound, thus decreasing fungal growth consequently it cannot form macro-aggregates. The obtained data were confirmed by **(Poznanski et al., 2023)** who found that CS is known for its strong anti-fungal efficacy. Also, it is biocompatible, biodegradable, and non-toxic. Because of its features, it has been frequently utilized to combat fungal pathogens.

For this reason, NCS encouraged the micro-aggregates formation more than macro-aggregates **(de Almeida et al., 2016; Soliman & Mansour, 2024)**. This result was confirmed by the positive correlation (r = 0.98) between the DOC (produced by NCS treatments after 14 days) and the amount of micro-aggregates <0.250 mm. This is consistent with what has been indicated by **(Yousefi et al., 2008)** where different SOC fractions have distinct functions in developing and maintaining soil aggregates. It observed different changes in TOC during 30 days of incubation, where NAG50% was the highest treatment for protecting TOC from microbial reactions, where the change rate of TOC was (0.15%) followed by NAG75% (0.97%) during the second period of incubation **(Fig. 8B)**. These results mean that TOC in soil treated with NAG loaded with NPKCa has stability compared with other CNPs and control treatment.
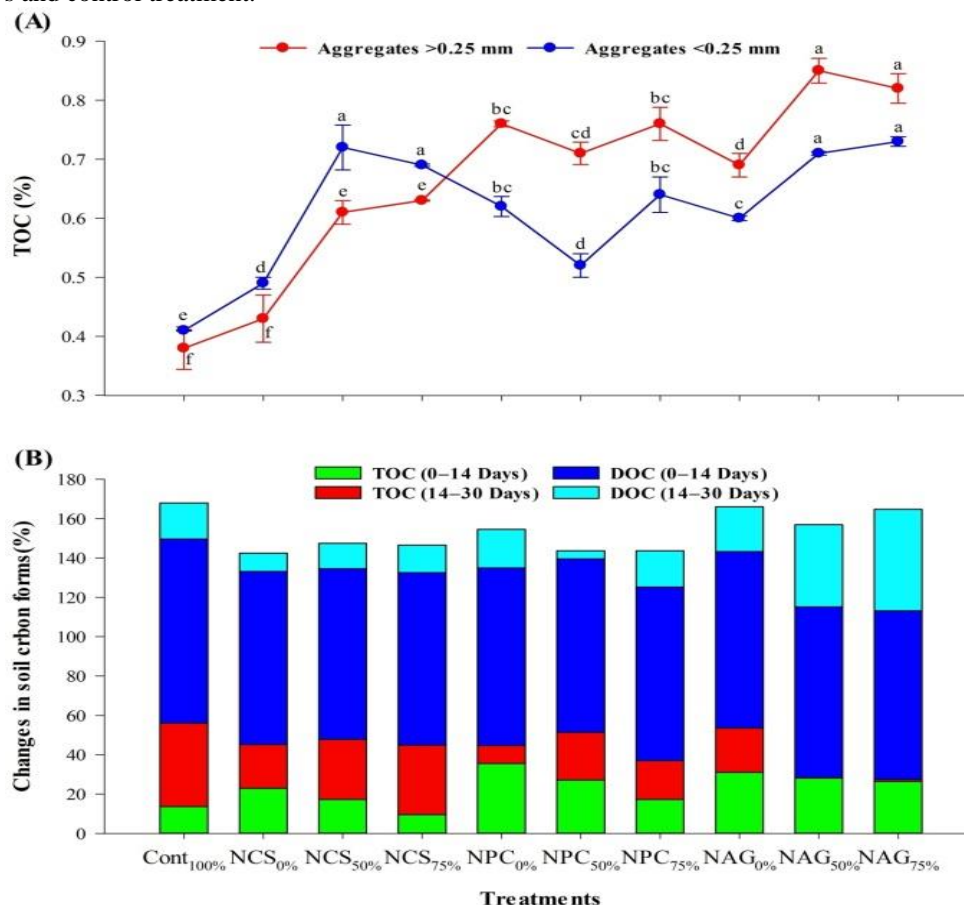
Fig. 8. Changes of SOC forms under different aggregates as affected by CNPs application.
Images show (A) The concentrations of TOC in aggregates less and more than 0.25 mm, and (B) the rate of changes in soil carbon forms with time, Cont: control, NCS: nano-chitosan, NPC: nano-pectin, NAG: nano-acacia gum, TOC: total organic carbon, DOC: dissolved organic carbon, LSD (0.05) for aggregates >0.25 and <0.25 mm = 0.022** and 0.029** respectively, Dissimilar letters were significantly different at $p<0.05$ according to the Duncan test, Bars on the curves stands for ± standard deviation (SD).

Contrary to expectations, CNPs application caused an increase in BD and a decrease in soil porosity, which differs from conventional organic matter in its effect on soil pores. Thus, CNPs can form macro-pores as a result of the formation of macro-aggregates rather than micro-aggregates, which reduces the soil volume and increases the BD value. Also, these results may be due to the coagulation force of AG overcoming the effect of OC. Although it reduces porosity, it increases MPD and thus increases water flow in studied soil **(Bayat et al., 2019; Koop et al., 2023; Soliman et al., 2019)**. Also, these results agree with **(Mestdagh et al., 2006; Sakin et al., 2011; Soliman & Mansour, 2024)** who reported that the direct correlation between BD and SOM is normal. Also, the addition of OM to clay loamy soil with high silt content will raise the BD of the soil and reduce porosity by increasing the proportion of macro-pores **(Soliman et al., 2019)**. In general, both micro-aggregation and macro-aggregation can be stimulated by increasing SOC content **(Halder et al., 2023; Plante & McGill, 2002)**.

The aggregation process in the soil is important, and it plays a considerable role in improving the soil's physical characteristics such as hydraulic conductivity, infiltration, aeration, etc. Also, the aggregation process is important in enhancing carbon sequestration in soil. The mean diameter of the CNPs increases with the addition of different electrolytes, indicating that the nutrients are being aggregated on the surface of CNPs. This search shows the effects of the application of CNPs on MWD as an index of aggregate formation and strength and organic carbon aggregate size fractions in degraded soil during the incubation period. The NAG was the perfect nanopolymer for high ZP and macro-aggregate formation, consequently, increasing the MWD, MPD and water flow through the studied soil. At that same time, the formation of soil aggregates protected the TOC from degradation. More studies are needed to understand and monitor the mechanism of SOC as an effective indicator in aggregate formation under different sizes, and textures for a long time.

5. Conclusions

Additional explorations need to be conducted to optimize the production of natural/biopolymeric-based (nano) materials to render them viable and sustainable towards industrial application. Aggregation of soil particles to macro- or micro-aggregates has been accomplished with the assistance of natural/biopolymeric-based carbon nanopolymers. Among polysaccharides, chitosan, pectin and gum are promising natural/biopolymers because of their sustainability, eco-friendly characteristics, reactivity, chemical stability, excellent physicochemical attributes, and considerable ability towards improve the soil structure, hydraulic properties, carbon sequestration and slow-release fertilizer all that makes them competitive the conventional agricultural practices. It derived from diverse derivatives is unquestionably the future wave of abundant resources that need to be exploited. Plentiful polysaccharides have been utilized for making assorted nanopolymers; fabrication of polysaccharides-supported carbon nanopolymers is one of the effective strategies in nanotechnology to face soil degradation which is considered one of the world's foremost food security concerns.

The nanopolymers produced showed spherical shapes and sizes of about 55.79, 29.38, and 49.53 nm for NCS, NPC, and NAG respectively using the TEM micrographs. The stability of the NPs colloidal suspension was influenced by the presence of the kinds from the urea, mono-potassium phosphate, and calcium chloride. The stability of the NPs colloidal suspension was higher with the addition of Ca than with the addition of NPK, due to the higher anion charge from the second than the first one. The average sizes of NPs-Ca50% recorded 17.90, 5.13, and 15.06 nm for NCS, NPC, and NAG respectively. The mean diameter increase of the CNPs with the addition of different compounds indicated that the nutrients are being aggregated on the surface of the NPs. NAG was the perfect nanopolymer for high zeta potential and macro-aggregate formation, consequently, increasing the MPD and water flow through the studied soil. At that same time, the formation of soil aggregates protected the TSOC from degradation. Further studies are needed to understand and monitor the mechanism of TSOC in aggregate formation under different sizes, and textures for a long time. Combating soil degradation is very essential and critical for safeguarding the environmental quality and maintaining life on the earth. As is clear from this search, emerging nanotechnologies have the potential to make carbon more effective where the aggregates could be related using relatively greener nanotechnology, but this field still needs extensive explorations; the major technical hurdle being their non-adaptability for industrial/large-scale systems and competitiveness to the traditionally deployed existing improvers options.

Availability of data and materials
All data presented or analyzed during this research are included in this published article.

Declarations

Ethics approval
All authors have read, understood, and have complied as applicable with the statement on "Ethical responsibilities of Authors" as found in the instructions for authors of the journal. Also, all soil and plant sampling procedures and standard methods were performed according to the relevant regulations and guidelines.

Consent for publication
Not applicable.

Competing interests
The authors declare that they have no conflicts of interest.

Abbreviations
AG: acacia gum, **CNPs:** carbon nanopolmers, **CS:** chitosan, **DOC:** dissolved organic carbon, **FTIR:** fourier transform infrared, **MAA:** methacrylic acid, **MPD:** mean pore diameter, **MWD:** mean weight diameter, **NAG:** nano-acacia, **NCS:** nano-chitosan, **NPC:** nano-pectin, **OC:** organic carbon, **OM:** organic matter, **PC:** pectin, **SOC:** soil organic carbon, **SOM:** soil organic matter, **TEM:** transmission electron microscope, **TOC:** total organic carbon.

References

Abd El-Halim, A. A. (2019). Effect of sugarcane pulp extract on ameliorating soil structure stability. *Egyptian Journal of Soil Science. 59*(3), 251–258. https://doi:10.21608/ejss.2019.13672.1279

Abdullatif, Y., Soliman, E., Hammad, S. A., El-Ghamry, A., & Mansour, M. M. (2024). Impact of carbon nanoparticles on aggregation and carbon sequestration under soil degradation – A review. *Journal of Soil Sciences and Agricultural Engineering, 15*(4), 85–92. https://dx.doi.org/10.21608/jssae.2024.278433.1223

Allam, M. A., Abd Elkawy, O. R., & Bahnassy, M. (2024). Effect of land use change on soil degradation and improvement in a dryland area in Egypt. *Egyptian Journal of Soil Science, 64*(4), 1697–1708. https://dx.doi:10.21608/ejss.2024.303260.1811

Baumert, V. L., Vasilyeva, N. A., Vladimirov, A. A., Meier, I. C., Kögel-Knabner, I., & Mueller, C. W. (2018). Root exudates induce soil macroaggregation facilitated by fungi in subsoil. *Frontiers in Environmental Science, 6*, 140. https://doi.org/10.3389/fenvs.2018.00140

Bayat, H., Kolahchi, Z., Valaey, S., Rastgou, M., & Mahdavi, S. (2019). Iron and magnesium nano-oxide effects on some physical and mechanical properties of a loamy Hypocalcic Cambisol. *Geoderma, 335*, 57–68. https://doi.org/10.1016/j.geoderma.2018.08.007

Beck-Broichsitter, S., Fleige, H., & Horn, R. (2018). Compost quality and its function as a soil conditioner of recultivation layers – a critical review. *International Agrophysics, 32*(1), 11–18. https://doi.org/10.1515/intag-2016-0093

Bronick, C. J., & Lal, R. (2005). Soil structure and management: a review. *Geoderma, 124*(1-2), 3–22. https://doi.org/10.1016/j.geoderma.2004.03.005

Castellano, M. J., Mueller, K. E., Olk, D. C., Sawyer, J. E., & Six, J. (2015). Integrating plant litter quality, soil organic matter stabilization, and the carbon saturation concept. *Global Change Biology, 21*(9), 3200–3209. https://doi.org/10.1111/gcb.12982

Corradini, E., de Moura, M. R., & Mattoso, L. H. C. (2010). A preliminary study of the incorparation of NPK fertilizer into chitosan nanoparticles. *Express Polymer Letters, 4*(8), 509–515. https://doi.org/10.3144/expresspolymlett.2010.64

Dane, J. H., & Topp, C. G. (2002). *Methods of soil analysis: Part 4 physical methods*. SSSA, Madison, WI, USA. https://doi.org/10.2136/sssabookser5.4

Das, B., Chakraborty, D., Singh, V. K., Aggarwal, P., Singh, R., & Dwivedi, B. S. (2014). Effect of organic inputs on strength and stability of soil aggregates under rice-wheat rotation. *International Agrophysics, 28*(2), 163–168. https://doi.org/10.2478/intag-2014-0004

de Almeida, F. T. R., Ferreira, B. C. S., da Silva Lage Moreira, A. L., de Freitas, R. P., Gil, L. F., & Gurgel, L. V. A. (2016). Application of a new bifunctionalized chitosan derivative with zwitterionic characteristics for the adsorption of Cu^{2+}, Co^{2+}, Ni^{2+}, and oxyanions of Cr^{6+} from aqueous solutions: Kinetic and equilibrium aspects. *Journal of Colloid and Interface Science, 466*, 297–309. https://doi.org/10.1016/j.jcis.2015.12.037

de Moura, M. R., Aouada, F. A., & Mattoso, L. H. C. (2008). Preparation of chitosan nanoparticles using methacrylic acid. *Journal of Colloid and Interface Science, 321*(2), 477–483. https://doi.org/10.1016/j.jcis.2008.02.006

Devaux, P. (2019, April 18). Egypt: The challenges of the agricultural sector. Eco Emerging, the Economic Research Portal, BNP Paribas, from https://economic-research.bnpparibas.com/html/en-US/challenges-agricultural-sector-4/18/2019,32926 (Accessed 24 June 2024)

Dielman, P. J., & De Ridder N. A. (1972). *Elementary ground water hydraulic*. Drainage Principle and Application Publication No. 16, ILRI, Wageningen, the Netherlands.

Dijkstra, F. A., Carrillo, Y., Pendall, E., & Morgan, J. A. (2013). Rhizosphere priming: a nutrient perspective. *Frontiers in Microbiology, 4*, 216. https://doi.org/10.3389/fmicb.2013.00216

Dohendou, M., Pakzad, K., Nezafat, Z., Nasrollahzadeh, M., & Dekamin, M. G. (2021). Progresses in chitin, chitosan, starch, cellulose, pectin, alginate, gelatin and gum based (nano)catalysts for the Heck coupling reactions: A review. *International Journal of Biological Macromolecules, 192*, 771–819. https://doi.org/10.1016/j.ijbiomac.2021.09.162

Durigan, M. R., Cherubin, M. R., De Camargo, P. B., Ferreira, J. N., Berenguer, E., Gardner, T. A., Barlow, J., Dias, C. T. d. S., Signor, D., Junior, R. C. d. O. & Cerri, C. E. P. (2017). Soil organic matter responses to anthropogenic forest disturbance and land use change in the Eastern Brazilian Amazon. *Sustainability, 9*(3), 379. https://doi.org/10.3390/su9030379

Elbasiouny, H., & Elbehiry, F. (2019). Soil carbon and nitrogen stocks and fractions for improving soil quality and mitigating climate change. *Egyptian Journal of Soil Science, 59*(2), 131–144. https://doi:10.21608/ejss.2019.9984.1251

El-Henawy, A. S., Khalifa, M. R., Gaheen, S. A., & El-Faramawy, H. (2024). Gypsum and nano-gypsum effects on certain soil characteristics and sorghum yield under saline-sodic soil conditions. *Egyptian Journal of Soil Science, 64*(3), 1009–1018. https://doi.org/10.21608/ejss.2024.283535.1749

Faizan, M., Alam, P., Rajput, V., Tonny, S., Yusuf, M., Sehar, S., Adil, M. F., & Hayat, S. (2023). Nanoparticles: an emerging soil crops saviour under drought and heavy metal stresses. *Egyptian Journal of Soil Science, 63*(3), 355–366. https://doi: 10.21608/ejss.2023.220619.1616

Garcia-Franco, N., Wiesmeier, M., Goberna, M., Martínez-Mena, M., & Albaladejo, J. (2014). Carbon dynamics after afforestation of semiarid shrublands: Implications of site preparation techniques. *Forest Ecology and Management, 319*, 107–115. https://doi.org/10.1016/j.foreco.2014.01.043

Gazzè, S. A., Saccone, L., Smits, M. M., Duran, A. L., Leake, J. R., Banwart, S. A., Ragnarsdottir, K. V. & McMaster, T. J. (2013). Nanoscale observations of extracellular polymeric substances deposition on phyllosilicates by an ectomycorrhizal fungus. *Geomicrobiology Journal, 30*(8), 721–730. https://doi.org/10.1080/01490451.2013.766285

Ghezzehei, T. A. (2012). Soil structure. In P. M. Huang, Y. Li, & M. E. Sumner (Eds.), *Handbook of soil sciences: Properties and processes* (2nd ed., pp. 1–17). CRC Press, Boca Raton, FL, USA.

Guber, A. K., Pachepsky, Y. A., & Levkovsky, E. V. (2005). Fractal mass–size scaling of wetting soil aggregates. *Ecological Modelling, 182*(3-4), 317–322. https://doi.org/10.1016/j.ecolmodel.2004.04.008

Guo, Z., Zhang, L., Yang, W., Hua, L., & Cai, C. (2019). Aggregate stability under long-term fertilization practices: The case of eroded Ultisols of South-Central China. *Sustainability, 11*(4), 1169. https://doi.org/10.3390/su11041169

Halder, M., Ahmad, S. J., Rahman, T., Joardar, J. C., Siddique, M. A. B., Islam, M. S., Islam, M. U., Liu, S., Rabbi, S. & Peng, X. (2023). Effects of straw incorporation and straw-burning on aggregate stability and soil organic carbon in a clay soil of Bangladesh. *Geoderma Regional, 32*, e00620. https://doi.org/10.1016/j.geodrs.2023.e00620

He, Y., Yang, M., Huang, R., Wang, Y., & Ali, W. (2021). Soil organic matter and clay zeta potential influence aggregation of a clayey red soil (Ultisol) under long-term fertilization. *Scientific Reports, 11*(1), 20498. https://doi.org/10.1038/s41598-021-99769-w

Hillel, D. (1982). *Introduction to soil physics* (1st ed.). Academic Press, San Diego, CA, USA. https://doi.org/10.1016/C2009-0-03052-9

ISO 10694 (1995). Soil quality — determination of organic and total carbon after dry combustion "elementary analysis" (1st

ed.). Geneva, Switzerland. https://www.iso.org/standard/18782.html (Accessed 24 June 2024)

ISO 11464 (2006). Soil quality — pretreatment of samples for physico-chemical analysis (2nd ed.). Geneva, Switzerland. https://www.iso.org/standard/37718.html (Accessed 24 June 2024)

ISO 13878 (1998). Soil quality — Determination of total nitrogen content by dry combustion "elemental analysis" (1st ed.). Geneva, Switzerland. https://www.iso.org/standard/23117.html (Accessed 24 June 2024)

Jílková, V., Straková, P., & Frouz, J. (2020). Foliage C:N ratio, stage of organic matter decomposition and interaction with soil affect microbial respiration and its response to C and N addition more than C:N changes during decomposition. *Applied Soil Ecology, 152*, 103568. https://doi.org/10.1016/j.apsoil.2020.103568

Jones, D. L., & Willett, V. B. (2006). Experimental evaluation of methods to quantify dissolved organic nitrogen (DON) and dissolved organic carbon (DOC) in soil. *Soil Biology and Biochemistry, 38*(5), 991–999. https://doi.org/10.1016/j.soilbio.2005.08.012

Jozedaemi, E., & Golchin, A., (2024). Changes in aggregate-associated carbon and microbial respiration affected by aggregate size, soil depth, and altitude in a forest soil. *Catena 234*, 107567. https://doi.org/10.1016/j.catena.2023.107567

Karami, A., Homaee, M., Afzalinia, S., Ruhipour, H., & Basirat, S. (2012). Organic resource management: Impacts on soil aggregate stability and other soil physico-chemical properties. *Agriculture, Ecosystems & Environment, 148*, 22–28. https://doi.org/10.1016/j.agee.2011.10.021

Kaushik, M., Fraschini, C., Chauve, G., Putaux, J. L., & Moores, A. (2015). Transmission electron microscopy for the characterization of cellulose nanocrystals. In K. Maaz (Ed.), *The transmission electron microscope - Theory and applications* (pp. 130–163). IntechOpen Ltd., Rijeka, Croatia. https://doi.org/10.5772/60985

Khalifa, N. S., & Hasaneen, M. N. (2018). The effect of chitosan–PMAA–NPK nanofertilizer on *Pisum sativum* plants. *3 Biotech, 8*(4), 193. https://doi.org/10.1007/s13205-018-1221-3

Koop, A. N., Hirmas, D. R., Billings, S. A., Li, L., Cueva, A., Zhang, X., Wen, H., Nemes, A., Souza, L. F. T., Ajami, H., Flores, A. N., Rudick, A. K., Guthrie, A., Klamm, L. M., Unruh, M. & Sullivan, P. L. (2023). Is macroporosity controlled by complexed clay and soil organic carbon? *Geoderma, 437*, 116565. https://doi.org/10.1016/j.geoderma.2023.116565

Lal, R. (2015). Restoring soil quality to mitigate soil degradation. *Sustainability, 7*(5), 5875–5895. https://doi.org/10.3390/su7055875

Lal, R. (2020). Soil organic matter content and crop yield. *Journal of Soil and Water Conservation, 75*(2), 27A–32A. https://doi.org/10.2489/jswc.75.2.27A

León, J. D., & Osorio, N. W. (2014). Role of litter turnover in soil quality in tropical degraded lands of Colombia. *The Scientific World Journal, 2014*, 693981. https://doi.org/10.1155/2014/693981

Li, J., Yang, Z. l., Ding, T., Song, Y. J., Li, H. C., Li, D. q., Chen, S. & Xu, F. (2022). The role of surface functional groups of pectin and pectin-based materials on the adsorption of heavy metal ions and dyes. *Carbohydrate Polymers, 276*, 118789. https://doi.org/10.1016/j.carbpol.2021.118789

Liu, Q., Meki, K., Zheng, H., Yuan, Y., Shao, M., Luo, X., Li, X., Jiang, Z., Li, F. & Xing, B. (2023). Biochar application in remediating salt-affected soil to achieve carbon neutrality and abate climate change. *Biochar, 5*(1), 45. https://doi.org/10.1007/s42773-023-00244-8

Lorenz, K., & Lal, R. (2018). *Carbon sequestration in agricultural ecosystems* (1st ed.). Springer International Publishing, Cham, Switzerland. https://doi.org/10.1007/978-3-319-92318-5

Mansour, M. M., & Soliman, E. (2022). Dynamics of dissolved ions in the rhizosphere under flooded conditions. *Journal of Soil Science and Plant Nutrition, 22*(2), 1362–1376. https://doi.org/10.1007/s42729-021-00738-z

Mechri, M., Bouajila, K., Ziadi, N., Raza, T., Beltayef, H., Eash, N. S., Jedidi, N., Gharbi, A., Hashem, A. & Abd Allah, E. F. (2023). Soil aggregation and associated organic carbon and total nitrogen in a sandy loam soil under long-term tillage effects. *Agronomy, 13*(10), 2520. https://doi.org/10.3390/agronomy13102520

Menšík, L., Hlisnikovský, L., & Kunzová, E. (2019). The state of the soil organic matter and nutrients in the long-term field experiments with application of organic and mineral fertilizers in different soil-climate conditions in the view of expecting climate change. In M. L. Larramendy & S. Soloneski (Eds.), *Organic fertilizers - history, production and applications* (1st ed., pp. 23–42). IntechOpen, London, UK. https://doi.org/10.5772/intechopen.86716

Mestdagh, I., Lootens, P., Van Cleemput, O., & Carlier, L. (2006). Variation in organic-carbon concentration and bulk

density in Flemish grassland soils. *Journal of Plant Nutrition and Soil Science, 169*(5), 616–622. https://doi.org/10.1002/jpln.200521861

Mirzaei Aminiyan, M., Safari Sinegani, A. A., & Sheklabadi, M. (2015). Aggregation stability and organic carbon fraction in a soil amended with some plant residues, nanozeolite, and natural zeolite. *International Journal of Recycling of Organic Waste in Agriculture, 4*(1), 11–22. https://doi.org/10.1007/s40093-014-0080-0

Musa, H. H., Ahmed, A. A., & Musa, T. H. (2018). Chemistry, biological, and pharmacological properties of gum Arabic. In J. M. Mérillon, & K. G. Ramawat (Eds.), *Bioactive molecules in food, Reference series in phytochemistry* (pp. 1–18). Springer, Cham. https://doi.org/10.1007/978-3-319-54528-8_11-1

Nasrollahzadeh, M., Sajjadi, M., Iravani, S., & Varma, R. S. (2021). Starch, cellulose, pectin, gum, alginate, chitin and chitosan derived (nano)materials for sustainable water treatment: A review. *Carbohydrate Polymers, 251*, 116986. https://doi.org/10.1016/j.carbpol.2020.116986

Obalum, S. E., Chibuike, G. U., Peth, S., & Ouyang, Y. (2017). Soil organic matter as sole indicator of soil degradation. *Environmental Monitoring and Assessment, 189*(4), 176. https://doi.org/10.1007/s10661-017-5881-y

Onweremadu, E. U., Onyia, V. N., & Anikwe, M. A. N. (2007). Carbon and nitrogen distribution in water-stable aggregates under two tillage techniques in Fluvisols of Owerri area, southeastern Nigeria. *Soil and Tillage Research, 97*(2), 195–206. https://doi.org/10.1016/j.still.2007.09.011

Plante, A. F., & McGill, W. B. (2002). Soil aggregate dynamics and the retention of organic matter in laboratory-incubated soil with differing simulated tillage frequencies. *Soil and Tillage Research, 66*(1), 79–92. https://doi.org/10.1016/S0167-1987(02)00015-6

Poznanski, P., Hameed, A., & Orczyk, W. (2023). Chitosan and chitosan nanoparticles: Parameters enhancing antifungal activity. *Molecules, 28*(7), 2996. https://doi.org/10.3390/molecules28072996

Reynolds, W. D., Elrick, D. E., Youngs, E. G., Booltink, H. W. G. & Bouma, J. (2002). Saturated and field-unsaturated water flow parameters: Laboratory methods. In J. H. Dane, & C. G. Topp (Eds.), *Methods of soil analysis: Part 4 physical methods* (pp. 802–816). SSSA, Madison, WI, USA. https://doi.org/10.2136/sssabookser5.4.c31

Sakin, E., Deliboran, A., & Tutar, E. (2011). Bulk density of Harran plain soils in relation to other soil properties. *African Journal of Agricultural Research, 6*(7), 1750–1757. https://doi.org/10.5897/AJAR10.502

Schmidt, M. W. I., Torn, M. S., Abiven, S., Dittmar, T., Guggenberger, G., Janssens, I. A., Kleber, M., Kögel-Knabner, I., Lehmann, J., Manning, D. A. C., Nannipieri, P., Rasse, D. P., Weiner, S. & Trumbore, S. E. (2011). Persistence of soil organic matter as an ecosystem property. *Nature, 478*(7367), 49–56. https://doi.org/10.1038/nature10386

Sekaran, U., Sagar, K. L., & Kumar, S. (2021). Soil aggregates, aggregate-associated carbon and nitrogen, and water retention as influenced by short and long-term no-till systems. *Soil and Tillage Research, 208*, 104885. https://doi.org/10.1016/j.still.2020.104885

Shafiei-Sabet, S., Hamad, W. Y., & Hatzikiriakos, S. G. (2014). Ionic strength effects on the microstructure and shear rheology of cellulose nanocrystal suspensions. *Cellulose, 21*(5), 3347–3359. https://doi.org/10.1007/s10570-014-0407-z

Soliman, E. M., Saleh, M. I., & Hammad, S. A. (2019). Benefits of treated rice straw on soil hydraulic properties under saline-sodic irrigation water. *Journal of Soil Sciences and Agricultural Engineering, 10*(7), 415–421. https://dx.doi.org/10.21608/jssae.2019.53687

Soliman, E., & Mansour, M. M. (2024). Enhancing soil organic carbon content and water retention using polyvinyl alcohol cross-linked with chitosan and pectin. *Journal of Soil Science and Plant Nutrition, 24*(1), 791–803. https://doi.org/10.1007/s42729-023-01584-x

Stavi, I., Bel, G., & Zaady, E. (2016). Soil functions and ecosystem services in conventional, conservation, and integrated agricultural systems: A review. *Agronomy for Sustainable Development, 36*(2), 32. https://doi.org/10.1007/s13593-016-0368-8

Sulman, B. N., Moore, J. A. M., Abramoff, R., Averill, C., Kivlin, S., Georgiou, K., Sridhar, B., Hartman, M. D., Wang, G., Wieder, W. R., Bradford, M. A., Luo, Y., Mayes, M. A., Morrison, E., Riley, W. J., Salazar, A., Schimel, J. P., Tang, J. & Classen, A. T. (2018). Multiple models and experiments underscore large uncertainty in soil carbon dynamics. *Biogeochemistry, 141*(2), 109–123. https://doi.org/10.1007/s10533-018-0509-z

Theng, B. K. G. (2012). Polysaccharides. In B. K. G. Theng (Ed.), *Developments in clay science*, vol. 4 (2nd ed., pp. 351–390). Elsevier, Amsterdam, the Netherlands. https://doi.org/10.1016/B978-0-444-53354-8.00011-6

Tisdall, J. M., & Oades, J. M. (1982). Organic matter and water-stable aggregates in soils. *Journal of Soil Science, 33*(2), 141–163. https://doi.org/10.1111/j.1365-2389.1982.tb01755.x

Tripathi, R., Nayak, A. K., Bhattacharyya, P., Shukla, A. K., Shahid, M., Raja, R., Panda, B. B., Mohanty, S., Kumar, A. & Thilagam, V. K. (2014). Soil aggregation and distribution of carbon and nitrogen in different fractions after 41 years long-term fertilizer experiment in tropical rice–rice system. *Geoderma, 213*, 280–286. https://doi.org/10.1016/j.geoderma.2013.08.031

Vargas, G., Verdejo, J., Rivera, A., Suárez, D., Youlton, C., Celis-Diez, J. L., Le Bissonnais, Y., Dovletyarova, E. A. & Neaman, A. (2019). The effect of four calcium-based amendments on soil aggregate stability of two sandy topsoils. *Journal of Plant Nutrition and Soil Science, 182*(2), 159–166. https://doi.org/10.1002/jpln.201700562

Voltr, V., Menšík, L., Hlisnikovský, L., Hruška, M., Pokorný, E., & Pospíšilová, L. (2021). The soil organic matter in connection with soil properties and soil inputs. *Agronomy, 11*(4), 779. https://doi.org/10.3390/agronomy11040779

Walkley, A., & Black, I. A. (1934). An examination of the Degtjareff method for determining soil organic matter, and a proposed modification of the chromic acid titration method. *Soil Science, 37*(1), 29–38.

Wang, X., Qi, J. Y., Zhang, X. Z., Li, S. S., Latif Virk, A., Zhao, X., Xiao, X. P. & Zhang, H. L. (2019). Effects of tillage and residue management on soil aggregates and associated carbon storage in a double paddy cropping system. *Soil and Tillage Research, 194*, 104339. https://doi.org/10.1016/j.still.2019.104339

Xie, J., Gao, J., Cao, H., Li, J., Wang, X., Zhang, J., Meng, H., Hong, J., Li, T. & Xu, M. (2024). Calcium carbonate promotes the formation and stability of soil macroaggregates in mining areas of China. *Journal of Integrative Agriculture, 23*(3), 1034–1047. https://doi.org/10.1016/j.jia.2023.09.015

Yamaguchi, T., Takei, T., Yazawa, Y., Wong, M. T. F., Gilkes, R. J., & Swift, R. S. (2004). Effect of humic acid, sodium, and calcium additions on the formation of water-stable aggregates in Western Australian wheatbelt soils. *Australian Journal of Soil Research, 42*(4), 435–439. https://doi.org/10.1071/SR03053

Yousefi, M., Hajabbasi, M., & Shariatmadari, H. (2008). Cropping system effects on carbohydrate content and water-stable aggregates in a calcareous soil of Central Iran. *Soil and Tillage Research, 101*(1-2), 57–61. https://doi.org/10.1016/j.still.2008.06.003

Zhou, M., Liu, C., Wang, J., Meng, Q., Yuan, Y., Ma, X., Liu, X., Zhu, Y., Ding, G., Zhang, J., Zeng, X. & Du, W. (2020). Soil aggregates stability and storage of soil organic carbon respond to cropping systems on Black Soils of Northeast China. *Scientific Reports, 10*(1), 265. https://doi.org/10.1038/s41598-019-57193-1

Zhu, S., Sainju, U. M., Zhang, S., Tan, G., Wen, M., Dou, Y., Yang, R., Chen, J., Zhao, F. & Wang, J. (2024). Cover cropping promotes soil carbon sequestration by enhancing microaggregate-protected and mineral-associated carbon. *Science of The Total Environment, 908*, 168330. https://doi.org/10.1016/j.scitotenv.2023.168330